Crystal structure and physical properties of $^{243}AmPd_5Al_2$

J.-C. Griveau,[1] K. Gofryk,[1,2] D. Bouëxière,[1] E. Colineau,[1] and J. Rebizant[1]

[1]*European Commission, Joint Research Centre, Institute for Transuranium Elements, Postfach 2340, D-76125 Karlsruhe, Germany*

[2]*Los Alamos National Laboratory, Los Alamos, New Mexico 87545, USA*

(Received 13 January 2012; published 13 February 2012)

We report on the crystal structure, magnetic susceptibility, specific heat, and electrical and thermoelectrical properties of $AmPd_5Al_2$, the americium counterpart of the unconventional superconductor $NpPd_5Al_2$. $AmPd_5Al_2$ crystallizes into the $ZrNi_2Al_5$ type of structure with lattice parameters: $a = 4.1298$ Å and $c = 14.7925$ Å. Magnetic measurements of $AmPd_5Al_2$ indicate a paramagnetic behavior with no hint of magnetic ordering nor superconductivity down to 2 K. This aspect is directly related to its $5f^6$ electronic configuration with $J = 0$. The specific heat measurements confirm the nonmagnetic ground state of this compound. The low temperature electronic specific heat $\gamma_e \sim 20$ mJ mol^{-1} K^{-2} is clearly enhanced as compared to americium metal. All transport measurements obtained point to a metallic behavior in $AmPd_5Al_2$.

DOI: 10.1103/PhysRevB.85.085108 PACS number(s): 72.15.−v, 61.66.Dk, 75.20.En, 65.40.Ba

I. INTRODUCTION

The discovery of unconventional superconductivity in transuranium-based intermetallics such as $PuCoGa_5$ (Ref. 1) and $PuRhGa_5$ (Ref. 2) has lead the scientific community to investigate the properties of numerous transuranium compounds, especially at low temperatures. $NpPd_5Al_2$ (Ref. 3) is the third transuranium and the first neptunium-based superconductor discovered within the last few years. Despite the fact that superconducting properties of $NpPd_5Al_2$ (Refs. 3–5) are analogous to $4f$ or $5f$ well studied Ce- or U-based heavy fermion superconductors,[6] there are still many open questions that have not been resolved, such as the pairing mechanism and the symmetry of the order parameter. In the case of transuranium-based superconductors, several scenarios were proposed recently to account for their superconductivity but the situation is still unclear [see Refs. 1 and 7–9]. While $NpPd_5Al_2$ is a heavy-fermion superconductor, the isostructural $ThPd_5Al_2$ (Ref. 10) and UPd_5Al_2 (Ref. 11) exhibit a paramagnetic ground state and $PuPd_5Al_2$ orders antiferromagnetically below 5.6 K (Ref. 10). The rare-earth (RE)-based compounds of the same structure, such as $CePd_5Al_2$ (Ref. 12) and $LuPd_5Al_2$ (Ref. 13), have also been examined, and some of them present fascinating features, such as pressure induced unconventional superconductivity.[14]

To explore further the f-electron properties and the richness of behavior intrinsically related to this $ZrNi_2Al_5$ structure, we have considered to substitute another transuranium element, namely americium. Americium (Am^{3+}) presents a nonmagnetic ground state due to its $5f^6$ electronic configuration ($J = 0$). In the case of americium metal, this implies a multitude of interesting properties, such as superconductivity[15] and an extreme sensitivity to external parameters like pressure[16] with a complex structural phase diagram.[17] It suggests then that an americium-based compound in this structure should present interesting properties.

Here we report on the crystal structure and magnetic, transport, and thermal properties of $AmPd_5Al_2$. It is worth noting the challenge and the difficulties when working with americium: it is a highly radioactive element and only one isotope allows low temperature studies (^{243}Am, $t_{1/2} = 7.38 \times 10^3$ yr, $Q = 6.3$ μW mg^{-1}). This isotope in its metal form at a quantity required for sample preparation (∼0.1 g scale) and physical property measurements is extremely rare. Such difficulties have generally prevented studies of americium-based intermetallics or compounds in the last decades especially those considering electrical transport properties (resistivity, magnetoresistance, and thermopower) and specific heat at low temperatures. This study constitutes therefore a clear advance on transplutonium basic properties at low temperatures. This should be added to the few ones reported[18,19] and would help to understand the nature of the unconventional superconductivity in $NpPd_5Al_2$, especially the magnetic fluctuation scenario related to $5f$ electrons.

II. EXPERIMENTAL

The polycrystalline samples were prepared by arc melting stoichiometric amounts of the pure metals components. Starting materials were used in the form of a 4N Pd pellet, 5N Al wire as supplied by A. D. Mackay Inc., and 99.85% Am metal (^{243}Am isotope[20]) produced originally by a thermoreduction process[21] with 3N purity. Other actinides (Np, Pu) are present at the ppm level[22] in Am after long term storage (∼10 yr). They do not contribute significantly to basic properties but decrease the purity level with time. Due to the contamination risk generated by the radiotoxicity of americium, all operations of preparation and encapsulation have been performed in gloveboxes under an inert N_2 atmosphere. Moreover the self-radiation and the self-damage induced by α disintegration constrain us to work very rapidly (within days). This aspect is even more drastic at low temperatures ($T < 10$ K). The arc melting was performed under a high purity argon atmosphere on a water-cooled copper hearth, using a Zr alloy as an oxygen/nitrogen getter. The arc-melted buttons were turned over and melted three times in order to ensure homogeneity. The weight losses after melting were smaller than 0.2%. The magnetic properties were determined using a Quantum Design (QD) MPMS-7 device in the temperature range 2–300 K and in magnetic fields up to 7 T. The heat capacity, electrical resistivity, and Hall effect were measured from 2.5 to 300 K with a QD PPMS-14 device up to 14 T on polycrystals. The thermoelectric power was measured from 3 to 300 K in a home-made setup using

pure copper as a reference material. For transport properties, all measurements have been determined by a four probe DC technique voltage measurement on a polycrystal sample polished on two opposite faces to present a flat surface with a typical size of $1 \times 0.4 \times 0.2$ mm^3. An electrical resistivity measurement has been performed with the applied current $I = 5$ mA along the flat surface, and the voltage V was extracted parallel to the current I while the applied magnetic field B was perpendicular to the flat surface for a magnetoresistivity determination. When applying a negative field at a fixed temperature, no parasitic Hall effect was observed for the magnetoresistivity. The Hall resistance R_H was determined by voltage measurements V_H under a field alternatively at $+14$ and -14 T. The field response $V_H(B)$ at fixed temperatures has been measured to confirm results obtained when ramping in the temperature. Excepting crystallographic structure determination, no orientation information related could be extracted from the basic properties observed.

III. CRYSTALLOGRAPHIC STRUCTURE

Small single crystals of typical size $50 \times 50 \times 20$ μm^3 suitable for crystal structure determination were mechanically extracted from the button and mounted inside a capillary for single crystal x-ray diffraction (Fig. 1, top). They were examined on an Enraf-Nonius CAD-4 diffractometer with the graphite monochromatized Mo $K\alpha$ radiation. The crystal structure that was solved by the direct method using the SHELX-97 (Ref. 23) and the data processing using the WINGX package[24] are reported in Table I. The atomic coordinates obtained are presented in Table II. The crystal structure was refined from the single-crystal x-ray data and was corrected for Lorentz and polarization effects. The results confirm the tetragonal unit cell. Samples were then examined by powder x-ray diffraction using a Bruker D8 diffractometer with the monochromated Cu $K\alpha_1$ radiation ($\lambda = 1.540\,59$ Å) equipped with a Vantec detector. The powder diffraction pattern (Fig. 2) was analyzed by a Rietveld profile refinement method[25] using the WINPLOTR-FULLPROF program.[26] Results are similar to those determined by x-ray single crystal diffraction, confirming the structure, the crystallographic parameters, and the good homogeneity of the polycrystals. Finally, the phase composition was determined by energy dispersive x-ray (EDX) analysis performed on a Philips XL40 scanning electron microscope (SEM). The microprobe analysis indicates good homogeneity (Fig. 1, bottom) for the samples and a single phase with stoichiometry close to 1:5:1.70 ($Am_{0.13}Pd_{0.65}Al_{0.22}$). This slight deficiency in aluminium on the bulk could be explained by the difficulty of integrating the Al signal vs Am. In conclusion, $AmPd_5Al_2$ adopts a tetragonal $ZrNi_2Al_5$ type of structure [space group (s.g.) $I4/mmm$] like $NpPd_5Al_2$ (Ref. 3) with lattice parameters $a = 4.1298(9)$ Å and $c = 14.792(4)$ Å.

IV. MAGNETIC PROPERTIES

The temperature dependence of the magnetic susceptibility of polycrystalline $AmPd_5Al_2$ is presented in Fig. 3. The compound shows a paramagnetic behavior with almost no temperature dependence down to 50 K. Below, an upturn leads to a slightly enhanced magnetic susceptibility at low

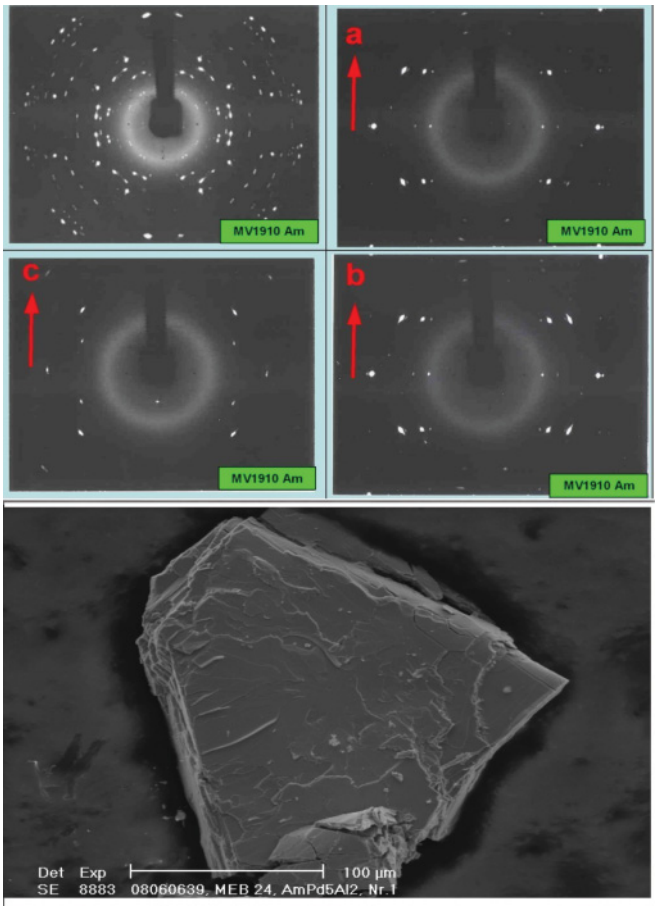

FIG. 1. (Color online) X-ray single crystal diffraction pattern obtained for a single crystal for a random orientation and along the main directions a, b, and c. (Bottom) energy dispersive x-ray (EDX) analysis performed on a polycrystal showing the homogeneity of the material.

temperatures with $\chi_{2\,\mathrm{K}} \sim 3.5 \times 10^{-3}$ emu mol^{-1}. A similar but weaker behavior has been reported for the magnetic susceptibility ^{241}Am metal[27] and is presented on the same figure for comparison. The field dependence of the magnetization, σ, taken at 5 K (see inset in Fig. 3) indicates a paramagnetic response. The nonmagnetic nature of $AmPd_5Al_2$ is expected from the ground state of americium ($5f^6$). In LS coupling the six $5f$ electrons of Am^{3+} will occupy the $J = 0$ state. In this case, due to the proximity of the first excited state $J = 1$, the susceptibility will mainly be governed by a Van Vleck term. On the other hand in the jj model, the six electrons will occupy the $j = 5/2$ subshell separated by spin-orbit coupling from the $j = 7/2$ sublevel. So, the susceptibility coming from a Pauli exchange reinforced term and an orbital contribution is rather anticipated. However, the exchange interactions are still present leading to an intermediate coupling of the $5f$ states. As has been shown in Am, an intermediate coupling is very close to the jj limit so only a small $5f$ electron occupation is observed in the $j = 7/2$ subband.[28,29] Therefore, the enhanced susceptibility values obtained for $AmPd_5Al_2$ compared to americium metal may come from a stronger Van Vleck contribution and/or Pauli paramagnetism. The presence of Pu and more specifically Np atoms created during the

TABLE I. Crystallographic data for $^{243}AmPd_5Al_2$ obtained from a single crystal.

Composition	$^{243}AmPd_5Al_2$
Space group	$I4/mmm$ (No. 139)
Lattice parameters (Å)	$a = 4.1298(9)$
	$c = 14.792(4)$
Cell volume(Å^3)	252.29
Formula units per cell	$Z = 2$
Formula mass	829.07
Calculated density (g/cm^3)	10.91
Crystal size (mm^3)	$0.03 \times 0.20 \times 0.05$
Radiation	Mo K_α ($\lambda = 0.710\,73$ Å)
Scans up to 2θ	70 °
Linear absorption coefficient	32.00 mm^{-1}
Total number of reflections	1008
	Unique: 201 ($R_F = 0.118$)
Reflections with $F_o > 4\sigma(F_o)$	154
Goodness of fit	1.134
Conventional residual R	0.0772 ($F > 4\sigma$)

long term storage could be considered but can not explain quantitatively the behavior at low temperatures. They can be present in the material, participating to a relative local disorder in the lattice without signatures on the x-ray powder diffraction patterns or EDX measurements. No sign of superconductivity nor magnetic order has been observed down to 2 K in $AmPd_5Al_2$.

V. TRANSPORT PROPERTIES

A. Electrical resistivity

The electrical resistivity and magnetoresistance of polycrystalline samples of $AmPd_5Al_2$ are presented in Fig. 4. The overall behavior of the electrical resistivity of $AmPd_5Al_2$ is clearly metallic with a relatively high value of the residual resistivity ρ_0 and a low value of the residual resistivity ratio ($r_R = 1.35$). The electrical resistivity value is small and points to the absence of magnetic scattering phenomena, such as Kondo or Ruderman-Kittel-Kasuya-Yosida (RKKY) interactions. It is interesting to note the similarity of behavior for all $4f$ and $5f$ counterparts $(RE,A)Pd_5Al_2$ with electrical resistivity ρ_{300K} around 15–30 $\mu\Omega$ cm (Refs. 5,10 and 12). Only $NpPd_5Al_2$ presents a higher electrical resistivity at room temperature ~90 $\mu\Omega$ cm (Refs. 3 and 4).

TABLE II. Crystallographic parameters for $^{243}AmPd_5Al_2$ obtained by single crystal x-ray diffraction. The structure was refined with anisotropic displacement parameters for all atoms. The last column contains the equivalent isotropic U values (Å^2).

Atom	Site	x	y	z	U_{eq}
Am	2a	0	0	0	0.0060
Pd1	8g	0.5	0	0.1453(2)	0.0069
Pd2	2b	0.5	0.5	0	0.0056
Al	4e	0	0	0.2545(20)	0.0106

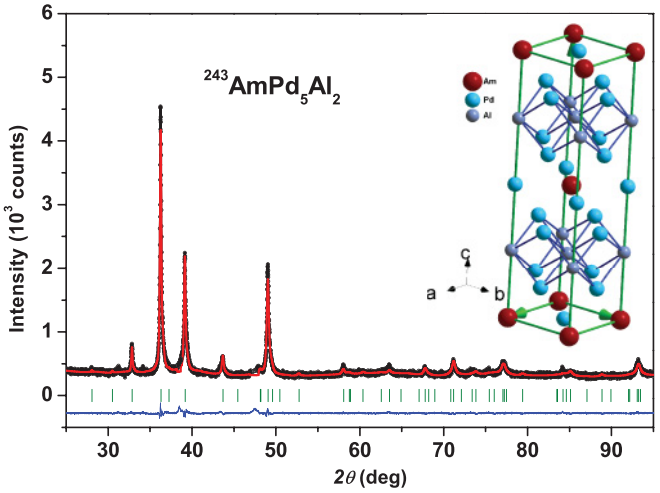

FIG. 2. (Color online) X-ray powder diffraction pattern ($\lambda = 1.540\,59$ Å) recorded for $^{243}AmPd_5Al_2$. The solid red line through the experimental points is the Rietveld refinement profile calculated for tetragonal $AmPd_5Al_2$. The blue line (bottom) corresponds to the difference between the measured and calculated Rietveld refinement. The crystal structure with the $ZrNi_2Al_5$ unit cell and the crystallographic parameters $a = 4.1298(9)$ Å and $c = 14.792(4)$ Å are presented.

Assuming the validity of Matthiessens rule, the resistivity of a nonmagnetic metallic compound should follow the Bloch-Grüneisen-Mott relation:[30–32]

$$\rho(T) = \rho_0 + 4R\Theta_R\left(\frac{T}{\Theta_R}\right)^5 \int_0^{\frac{\Theta_R}{T}} \frac{x^5 dx}{(e^x - 1)(1 - e^{-x})} - KT^3, \quad (1)$$

where Θ_R is the Debye temperature obtained by resistivity and R is a constant, whereas the third term KT^3 describes

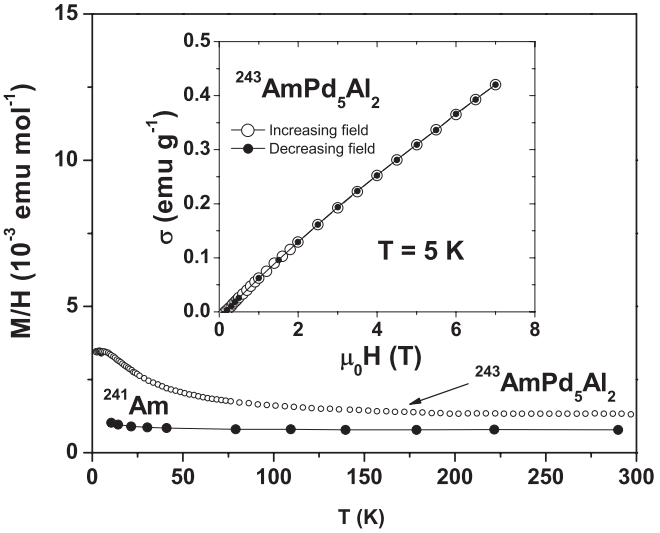

FIG. 3. Temperature dependence of the magnetic susceptibility M/H of $^{243}AmPd_5Al_2$ for $H = 70$ kOe. The magnetic susceptibility reported by Kanellakopoulos *et al.*[27] for ^{241}Am metal is also plotted on the graph. Inset: Magnetization σ measured at 5 K for an increasing and decreasing magnetic field H. The value is very small even at the highest applied magnetic field (~0.4 emu g^{-1}).

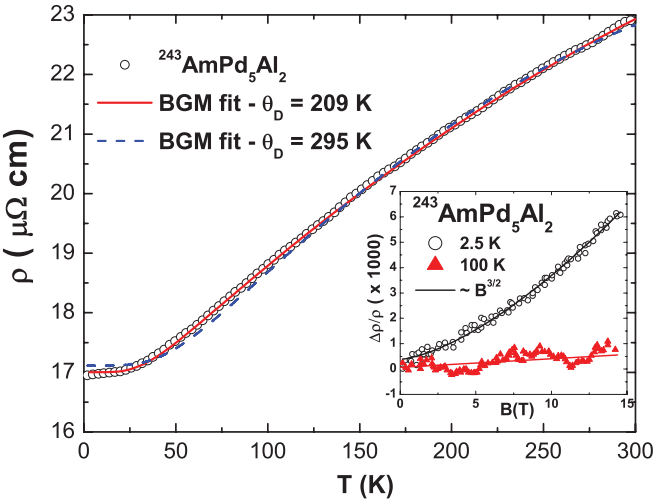

FIG. 4. (Color online) The temperature dependence of the electrical resistivity of $AmPd_5Al_2$. Two adjustments by the Bloch-Gruneisen model (BGM) are presented, with Θ_D as a free parameter (red full line) and equal to 295 K (blue dash line). Inset: magnetoresistivity taken at 2.5 and 100 K up to 14 T. A $B^{3/2}$ regime is visible at 2.5 K.

interband electron scattering processes on the *s*-*d* bands in the case of transition metal alloys and *s*-*f* bands in the case of *f* metals. The magnitude of the constant K and its sign depend on the density of states at the Fermi level. The adjustment of the electrical resistivity curve by a Linear Square Fit as shown in Fig. 4 according to Eq. (1) gives the following results: residual resistivity $\rho_0 = 17.0\ \mu\Omega\,\mathrm{cm}$, phonon scattering term $R = 2.372 \times 10^{-2}\mu\Omega\,\mathrm{cm\,K^{-1}}$, Debye-temperature $\Theta_R = 209$ K, and scattering coefficient of the conduction electrons into a narrow *d* band near the Fermi level $K = 2.978 \times 10^{-8}\ \mu\Omega\,\mathrm{cm\,K^{-3}}$. This value of Debye temperature is roughly of the same order of magnitude as obtained by the heat capacity (200–300 K) but slightly reduced. A second fit using the Debye temperature obtained by heat capacity measurements ($\Theta_D = 295$ K, see Sec. IV) is presented on the same figure (Fig. 4). The values are then $\rho_0 = 17.1\ \mu\Omega\,\mathrm{cm}$, $R = 2.50 \times 10^{-2}\ \mu\Omega\,\mathrm{cm\,K^{-1}}$, and $K = 5.18 \times 10^{-8}\ \mu\Omega\,\mathrm{cm\,K^{-3}}$. This fit does not reproduce well the overall shape of the electrical resistivity especially at low temperatures. The discrepancy between the two fits can be explained by two origins.

On one side, the different phonons branches contribute differently to the two properties (heat capacity and electronic transport). The electrical conductivity ($\sigma \sim 1/\rho$) is predominantly limited by the interaction between conduction electrons and longitudinal phonons, whereas the low temperature specific heat is dominated by transverse phonons.[33] This is clearly reinforced in the case of anisotropic structures presenting highly selective modes.

On the other side, the r_R can be reduced by the disorder created by the Am decay. We suggest considering an increased interaction at low temperatures of some defects induced by self-disintegration of Am atoms creating Frenkel pairs in the lattice. These defects appear quite fast despite the short delay between synthesis and measurement (within a week) and play a much stronger role than the presence of Np and Pu atoms created during long term storage that should not contribute significantly to the transport properties as from the magnetization. They could lead to an "impurity effect" with time, reducing the r_R as their effect is even more visible at low temperatures when phonon modes are reduced. This phenomenon has been clearly observed in intermetallic systems especially in the case of superconductors.[9]

We get the same value for the residual resistivity ρ_0 for both adjustments but slightly enhanced values for R and K contants for the $\Theta_R = 209$ K case. The R constant is of the same order of magnitude as nonmagnetic $5f$ (Ref. 34) or localized/mixed valence $4f$ intermetallics $\sim 10^{-2}\ \mu\Omega\,\mathrm{cm\,K^{-1}}$, such as $YbTIn_5$ (T = Rh,Ir) (Ref. 35) and $YbAl_2$ (Ref. 36), but the K constant is clearly reduced by one or two orders of magnitude ($10^{-8}\mu\Omega$ cm $\mathrm{K^{-3}}$ for $AmPd_5Al_2$) in comparison to $UTGa_5$ (T = Co,Rh), for instance ($\sim 10^{-6}\mu\Omega$ cm $\mathrm{K^{-3}}$ for $URhGa_5$) (Ref. 37). As the value of K as well as its sign depend on the density of states at the Fermi level, this illustrates the localized aspect of the material and the absence of $5f$ electrons at the Fermi level.

The inset in Fig. 4 presents the magnetoresistivity (MR) data $\Delta\rho/\rho \times 1000$ taken at 2.5 and 100 K using black circle and red triangles, respectively. As may be seen from the figure, we observe, in $AmPd_5Al_2$, an extremely small positive magnetoresistivity (<1%). At 2.5 K the field dependence of the resistivity may be well described by a power law behavior $B^{3/2}$ (see the solid line in the inset of Fig. 4). It is slightly different from $\rho(B)$ observed in pure simple metals where resistivity grows quadratically with the field.[32] This can be related to the large anisotropy of the cristallographic structure as reported for other counterparts of the 1:5:2 family[3,13] and by the "impurity effect."[38] This impurity effect is noticeable on magnetotransport because all other contributions are negligible: the $5f$ electrons are localized and are not participating in the bonding. The small positive values of MR points to closed $5f$ shell characteristics. Only remaining *s*,*p*,*d* electrons can interact and lead to a scattering effect noticeable on the metallic-like shape of the material and on the weak magnetotransport properties. To estimate the electronic carriers qualitatively and quantitatively, we have performed Hall and Seebeck effect measurements.

B. Hall and Seebeck effects

The temperature dependence of the Hall coefficient R_H measured in a magnetic field of 14 T is shown in Fig. 5. R_H is positive up to 70 K where it changes sign to negative. Unlike simple metals, R_H of $AmPd_5Al_2$ is strongly temperature dependent. This could suggest, in $AmPd_5Al_2$ the presence of a complex electronic structure with multiple electron and hole bands with different temperature variations of carrier concentrations and mobilities. The higher value of the Hall effect at low temperatures could come from the reduction of the carrier mobility when going down to 0 K. Above 100 K the R_H is of the order of $-2 \times 10^{-10}\ \mathrm{m^3\,C^{-1}}$, which corresponds in a one band model to the effective electron concentration $n_{\mathrm{Hall}} \sim 3.2 \times 10^{22}\ \mathrm{cm^{-3}}$. It agrees well with the thermoelectric data (see below).

The inset of Fig. 5 shows the temperature dependence of the thermoelectric power of $AmPd_5Al_2$. It is worth noting that, up to our best knowledge, it is the first measurement of the Seebeck coefficient of a Am-based system. The thermopower

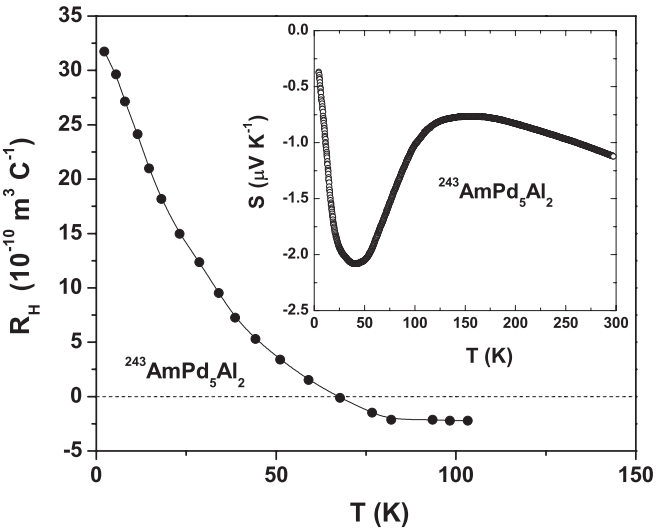

FIG. 5. The temperature dependence of the Hall effect and thermoelectric power (inset) of $AmPd_5Al_2$.

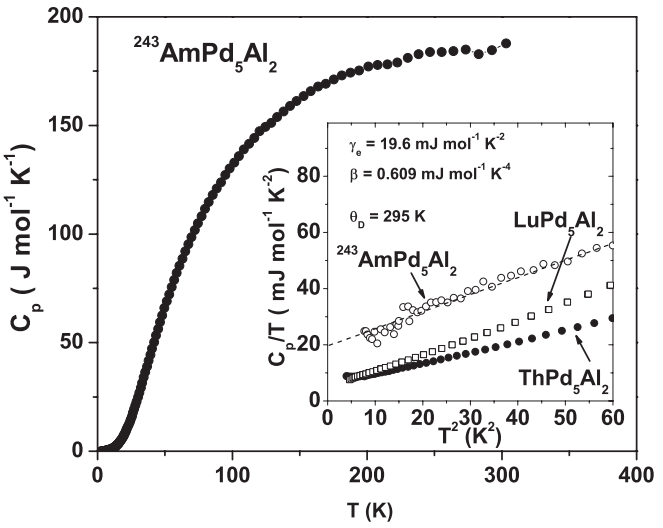

FIG. 6. The temperature dependence of the heat capacity of $AmPd_5Al_2$. Inset: low temperature specific heat of $AmPd_5Al_2$ plotted as C_p/T vs T^2 (see text).

is negative in the whole temperature range suggesting the dominant role of electrons in the electrical and heat conduction. The low-temperature dependence of the thermoelectric power $S(T)$ shows a clear extremum at $T_{\rm ext} = 45$ K. Then, with decreasing temperature, S decreases down to zero when $T \to 0$ K, as expected. This extremum of the thermopower can be related to the phonon drag effect, where the position is a measure of the Debye temperature [$\Theta_D \approx T_{\rm ext}/5$ (see Ref. 39)], which we estimate for $AmPd_5Al_2$ to be of about 230 K. It is of the same order as Θ_D values estimated from the electrical resistivity and specific heat measurements (see below). Above 150 K the thermopower is roughly proportional to the temperature, hence indicating that the main contribution to $S(T)$ comes from the diffusion of the carriers due to the applied temperature gradient. This mechanism is generally expressed as[39]

$$S(T) = \frac{k_{\rm B}^2 \pi^2 T}{3eE_{\rm F}}. \qquad (2)$$

Within a single-band model the value of the thermoelectric power measured at room temperature (-1.1 μV K^{-1}) implies the Fermi energy and effective carrier concentrations to be about $E_{\rm F} = 6.5$ eV and $n_{\rm Seebeck} \sim 7.5 \times 10^{22}$ cm^{-3}, respectively. The value of n is very close to the one obtained from the Hall effect measurements and is also similar to n observed in usual metals, such as Al or Cu (Refs. 32 and 40). However, taking into account the simplicity of the model applied, the estimated carrier concentration could account for the upper limit of the carrier concentration in $AmPd_5Al_2$. Altogether, it strongly suggests the absence of $5f$ electrons in the electronic properties: only s-p-d carriers participate in the bonding while $5f$ electrons are well localized in $AmPd_5Al_2$.

VI. HEAT CAPACITY

The specific heat measurements of $AmPd_5Al_2$ are presented on Fig. 6. The absence of magnetic order and/or superconductivity in this system down to 3 K is clearly confirmed. Near room temperature C_p has a value of about 180 J mol^{-1} K^{-1} which is slightly lower than the Dulong-Petit limit, i.e., $C_p = 3rR = 199$ J/mol K, where r is the number of atoms per molecule and R is the gas constant. The low temperature part of the specific heat allows us to determine the electronic contribution γ_e and Debye temperature θ_D by a linear fit of $C_p/T \sim \gamma_e + \beta T^2$, with β related to θ_D (see inset of Fig. 6). For $AmPd_5Al_2$ we get $\gamma_e = 19$ mJ mol^{-1} K^{-2} and $\theta_D = 295$ K. The value of θ_D is very close to the other nonmagnetic counterparts of the family, $\theta_D = 290$ K for $ThPd_5Al_2$ and 310 K for $LuPd_5Al_2$. The value of γ_e obtained is relatively enhanced especially when compared to americium metal[41] or to other classical metals. However this value is much smaller than all other parent compounds of the $ZrNi_2Al_5$ structure [325 mJ mol^{-1} K^{-2} for $NpPd_5Al_2$ (Ref. 5) and 61 mJ mol^{-1} K^{-2} for $PuPd_5Al_2$ (Ref. 10)] and is rather close to the one for $ThPd_5Al_2$ (4.4 mJ mol^{-1} K^{-2}) as this latter one does not present any $5f$ contribution. It suggests the presence of well localized $5f$ electrons in $AmPd_5Al_2$. The slight enhancement of γ_e could come from the $5d$–$6d$ exchange correlations between Pd and Am atoms. However, further measurements using synchrotron techniques as magnetic x-ray circular dichroism are needed to reach conclusions on this point.

VII. DISCUSSION AND CONCLUSION

In conclusion, the Am-based intermetallic compound $AmPd_5Al_2$ crystallizes, like other members of the $AnPd_5Al_2$ family in the tetragonal $ZrNi_2Al_5$ type of structure (s.g. $I4/mmm$) with lattice parameters $a = 4.1298(9)$ Å and $c = 14.793(4)$ Å, as determined by single crystal studies. The magnetic measurements revealed that $AmPd_5Al_2$ shows a temperature independent paramagnetic behavior, enhanced compared to Am metal. In agreement with the electronic configuration of americium, it does not show any hint of a magnetic nor superconducting signature down to 2 K. The nonmagnetic ground state, governed by the $J = 0$ configuration, is also supported by specific heat measurements. The electrical

resistivity, Hall effect, and thermoelectric power are characteristic of a good metallic system with the carrier concentration of the order of 10^{22} cm^{-3}. This clearly point to the presence in $AmPd_5Al_2$ of well localized $5f$ electrons. Moreover, the absence of superconductivity in this system strongly emphasizes the importance of magnetic interactions as a possible medium of the unconventional superconductivity in $NpPd_5Al_2$. Electronic structure calculations would be of great interest to determine the position of $5f$ states vs the Fermi energy in $AmPd_5Al_2$ and compare it to the other members of the $(RE,A)Pd_5Al_2$ family.

ACKNOWLEDGMENTS

We are grateful to H. Thiele for technical assistance for the EDX analysis. K.G. acknowledges the European Commission for support in the frame of the "training and Mobility of Researchers" program.

[1] J. L. Sarrao, L. A. Morales, J. D. Thompson, B. L. Scott, G. R. Stewart, F. Wastin, J. Rebizant, P. Boulet, E. Colineau, and G. H. Lander, Nature (London) **420**, 297 (2002).
[2] F. Wastin, P. Boulet, J. Rebizant, E. Colineau, and G. H. Lander, J. Phys. Cond. Matter **28**, 2279 (2003).
[3] D. Aoki, Y. Haga, T. D. Matsuda, N. Tateiwa, S. Ikeda, Y. Homma, H. Sakai, Y. Shiokawa, E. Yamamoto, A. Nakamura, R. Settai, and Y. Onuki, J. Phys. Soc. Jpn. **76**, 063701 (2007).
[4] J.-C. Griveau, K. Gofryk, and J. Rebizant, Phys. Rev. B **77**, 212502 (2008).
[5] K. Gofryk, J.-C. Griveau, E. Colineau, J. P. Sanchez, J. Rebizant, and R. Caciuffo, Phys. Rev. B **79**, 134525 (2009).
[6] G. R. Stewart, Rev. Mod. Phys. **73**, 797 (2001).
[7] N. J. Curro, T. Caldwell, E. D. Bauer, L. A. Morales, M. J. Graf, Y. Bang, A. V. Balatsky, J. D. Thompson, and J. L. Sarrao, Nature (London) **434**, 622 (2005).
[8] Y. Bang, A. V. Balatsky, F. Wastin, and J. D. Thompson, Phys. Rev. B **70**, 104512 (2004).
[9] F. Jutier, G. A. Ummarino, J.-C. Griveau, F. Wastin, E. Colineau, J. Rebizant, N. Magnani, and R. Caciuffo, Phys. Rev. B **77**, 024521 (2008).
[10] K. Gofryk, J.-C. Griveau, E. Colineau, and J. Rebizant, Phys. Rev. B **77**, 092405 (2008).
[11] Y. Haga, T. D. Matsuda, S. Ikeda, E. Yamamoto, N. Duc Dung, and Y. Onuki, J. Phys. Soc. Jpn. Suppl. A **77**, 365 (2008).
[12] R. A. Ribeiro, Y. F. Inoue, T. Onimaru, M. A. Avila, K. Shigetoh, and T. Takabatake, Physica B **404**, 2946 (2009).
[13] R. de A. Ribeiro, T. Onimaru, K. Umeo, M. de A. Avila, K. Shigetoh, and T. Takabatake, J. Phys. Soc. Jpn. **76**, 123710 (2007).
[14] F. Honda, M.-A. Measson, Y. Nakano, N. Yoshitani, E. Yamamoto, Y. Haga, T. Takeuchi, H. Yamagami, K. Shimizu, R. Settai, and Y. Onuki, J. Phys. Soc. Jpn. **77**, 043701 (2008).
[15] J. L. Smith and R. G. Haire, Science **200**, 535 (1978).
[16] J.-C. Griveau, J. Rebizant, G. H. Lander, and G. Kotliar, Phys. Rev. Lett. **94**, 097002 (2005).
[17] S. Heathman, R. G. Haire, T. Le Bihan, A. Lindbaum, K. Litfin, Y. Méresse, and H. Libotte, Phy. Rev. Lett. **85**, 2961 (2000).
[18] P. Javorský, F. Wastin, E. Colineau, J. Rebizant, P. Boulet, and G. R. Stewart, J. Nucl. Mater. **344**, 50 (2005).
[19] J.-C. Griveau, J. Rebizant, F. Wastin, E. Colineau, F. Jutier, and G. H. Lander, MRS Proc. (2005) **893**, 0893 (2006).
[20] W. Müller and J.-C. Spirlet, in *Actinides—Chemistry and Physical Properties*, Structure and Bonding, Vol. 59/60 (Springer-Verlag Berlin, Heidelberg, 1985), p. 57.
[21] J.-C. Spirlet and W. Müller, J. Less-Common Met. **31**, 35 (1973).
[22] W. Müeller, R. Schenkel, H. E. Schmidt, J. C. Spirlet, J. C. McElroy, D. L. Hall, and M. J. Mortimer, J. Low Temp. Phys. **30**, 561 (1978).
[23] G. M. Sheldrix, computer code SHELX-97 (Universität Göttingen, 1997).
[24] L. J. Farrugia, J. Appl. Crystallogr. **32**, 837 (1999).
[25] H. M. Rietveld, J. Appl. Crystallogr. **2**, 65 (1969).
[26] T. Roisnel and J. Rodríguez-Carvajal, Mater. Sci. Forum **378**, 118 (2001).
[27] B. Kanellakopulos, A. Blaise, J. M. Fournier, and W. Müller, Solid State Commun. **17**, 713 (1975).
[28] S. Y. Savrasov, K. Haule, and G. Kotliar, Phys. Rev. Lett. **96**, 036404 (2006).
[29] Kevin T. Moore and Gerrit van der Laan, Rev. Mod. Phys. **81**, 235 (2009).
[30] N. F. Mott and H. Jones, *The Theory of the Properties of Metals and Alloys* (Oxford University Press, London, 1936), p. 268.
[31] G. Grimvall, *The Electron-Phonon Interaction in Metals* (North Holland, Amsterdam, 1981).
[32] T. G. Berlincourt, Phys. Rev. **112**, 381 (1958).
[33] C. Enss and S. Hunklinger, *Low-Temperature Physics* (Springer, Heidelberg, 2005), p. 175.
[34] R. Troć, Z. Bukowski, C. Sułkowski, H. Misiorek, J. A. Morkowski, A. Szajek, and G. Chełkowska, Phys. Rev. B **70**, 184443 (2004).
[35] Z. Bukowski, K. Gofryk, and D. Kaczorowski, Solid State Commun. **134**, 475 (2005).
[36] H. Nowatari, Y. Saiga, Y. Kato, K. Iwata, S. Katano, T. Fujiwara, Y. Uwatoko, and M. Kosaka, J. Phys. Soc. Jpn. Suppl. A **76**, 80 (2007).
[37] R. Wawryk, Z. Henkie, T. Cichorek, C. Geibel, and F. Steglich, Phys. Status Solidi **232**, R4 (2002).
[38] T. Graf, R. Movshovich, J. D. Thompson, Z. Fisk, and P. C. Canfield, Phys. Rev. B **52**, 3099 (1995).
[39] F. Blatt, P. Schroeder, C. Foiles, and D. Greig, *Thermoelectric Power of Metals* (Plenum, New York, 1976).
[40] S. Foner, Phys. Rev. **107**, 1513 (1957).
[41] J. L. Smith, G. R. Stewart, C. Y. Huang, and R. G. Haire, J. Phys. (Paris), Colloq. **40**, C4–138 (1979).